Cation distribution in the octahedral sites of hornblendes

Kuniaki Makino, Katsutoshi Tomita

Department Geology and Mineralogy, Kyoto University, Kyoto 606, Japan

Abstract

The structure refinements of five calcic amphiboles with $^{[4]}Al > 0.5$ have been carried out in order to characterize the cation distributions in the octahedral sites in amphiboles formed at different temperatures. The location and atomic fractions of Al and Fe^{3+} in the octahedral M(1), M(2), and M(3) sites were determined together with other constituent cations on the basis of the site refinement and the relations between mean bond length and mean ionic radius.

The studied specimens are two metamorphic pargasites, a volcanic pargasite, a volcanic magnesio-hornblende, and a hastingsite from a skarn. In the metamorphic pargasites and the hastingsite, Al, Fe^{3+}, and Ti occupy only the M(2) site, and Mg prefers the M(2) site to the M(1) and M(3) sites (Mg-Fe^{2+} partitioning; $K_D^{M(1)-M(2)} = 0.30$ between the M(1) and M(2) sites). On the other hand, the volcanic pargasite and hornblende indicate a more disordered cation distribution among the octahedral sites than that from metamorphic rocks and skarn.

Introduction

Calcic amphibole is an important rock-forming mineral and occurs in extremely wide varieties of metamorphic, plutonic, and volcanic rocks. A chemical discontinuity in the calcic amphiboles exists between Al-rich and Al-poor phases (e.g., Shido and Miyashiro, 1959; Yamaguchi et al., 1983). The Al-rich phase with $^{[4]}Al > 0.5$ is termed hornblende, subsuming the appropriate names for amphibole defined by Leake (1978), such as pargasite, tschermakite, and actinolitic hornblende.

The basic structural unit in calcic amphibole is a double chain of TO_4 tetrahedra extending parallel to the *c* axis (Warren, 1929, 1930). The octahedral cation strips are sandwiched between the double chains. There are two distinct tetrahedral sites, T(1) and T(2), which contain Si and Al. The octahedral sites are subdivided into three crystallographically nonequivalent sites, M(1), M(2), and M(3), which accommodate various cations such as Mg, Fe^{2+}, Mn, Fe^{3+}, Al, and Ti. The M(4) site accommodates Ca, Na, Mg, and Fe^{2+}. A large A site may be vacant or may contain Na and K cations.

Using data obtained from modern techniques, the geometry and chemistry of the cation sites in hornblendes have been discussed in detail (Papike et al., 1969; Kitamura et al., 1975; Robinson et al., 1973; Hawthorne and Grundy, 1973; Hawthorne et al., 1980; Ungaretti et al., 1981). The stereochemistry of the tetrahedral double chains and the octahedral strips in the $C2/m$ amphibole was summarized by Hawthorne (1981, 1983).

Papike et al. (1969) observed the preference of Al for the T(1) site relative to the T(2) site in hornblendes based on the ⟨T(1)–O⟩ and ⟨T(2)–O⟩ lengths. The correlation between the Al content and the mean bond length of the

tetrahedral sites in calcic amphiboles was demonstrated by Robinson et al. (1973) and Hawthorne and Grundy (1977).

Finding the ordering of trivalent cations at the smaller M(2) site in Bolivian crocidolite (magnesio-riebeckite) (Whittaker, 1949) and in glaucophane (Papike and Clark, 1968) helped in understanding the crystal chemistry of the octahedral sites in hornblende; the smaller Al, Fe^{3+}, and Ti cations are confined to the M(2) site in hornblende, because it is usually much smaller than the M(1) and M(3) sites. Robinson et al. (1973) demonstrated that the mean bond lengths of the octahedral sites were a linear function of the mean ionic radius of the constituent cations. This relationship was extended to the grand octahedral site, which combines the M(1) site with the M(2) and M(3) sites, and to individual M(1), M(2), and M(3) sites of the $C2/m$ amphiboles by Hawthorne (1978, 1981, 1983).

In the metamorphic cummingtonites, the Ca-poor amphiboles with space group $C2/m$ or $P2_1/m$, the Mg-Fe^{2+} distribution between the M(4) site, and the M(1, 2, 3) site was discussed by Hafner and Ghose (1971). The temperature dependency of the Mg-Fe^{2+} distribution between the M(4) site and the M(1, 2, 3) site was suggested and discussed by Mueller (1962) and Ghose and Weidner (1972). The kinetics of the Mg-Fe^{2+} exchange reaction between the M(4) site and the M(1, 2, 3) site in an anthophyllite were discussed by Seifert and Virgo (1975).

On the contrary, the chemical complexity of hornblende has obscured the temperature dependency of its cation distribution. In particular, the site preference of Al (or other trivalent cations) in the octahedra at high temperature has not been studied. This study was undertaken to characterize the distribution of cations among the oc-

TABLE 1. Chemical composition of the hornblendes

	I-P	E-P	O-H	P-P	K-H
SiO_2	41.50	41.03	38.82	41.07	47.87
Al_2O_3	14.40	17.34	9.07	17.94	7.52
TiO_2	1.66	0.42	0.58	0.18	1.35
Fe_2O_3	—	1.96	5.57	3.59	—
FeO	12.60	5.04	25.87	7.79	12.74
MnO	0.12	0.0	0.25	0.14	0.43
MgO	11.88	14.39	1.91	13.37	15.30
CaO	10.65	12.71	11.79	12.05	10.95
Na_2O	3.22	1.21	2.79	1.83	1.29
K_2O	0.32	3.19	0.92	0.31	0.44
H_2O^+	—	1.15	2.31	1.46	—
H_2O^-	—	—	0.27	0.57	—
Cl	—	0.65	0.20	—	—
$-Cl \equiv O$	—	0.15	0.05	—	—
Total	96.35	98.94	100.30	100.30	97.89
Cations on the basis of 23 oxygens					
Si	6.19	5.99	6.31	5.92	6.90
Al	1.81	2.01	1.69	2.08	1.10
Σ [4]	8.00	8.00	8.00	8.00	8.00
Al	0.72	0.97	0.05	0.96	0.17
Ti	0.19	0.05	0.07	0.02	0.14
Fe^{3+}	0.05*	0.22	0.68	0.39	0.43*
Fe^{2+}	1.52	0.62	3.52	0.94	1.11
Mn	0.02	0.0	0.03	0.03	0.05
Mg	2.64	3.13	0.47	2.87	3.29
Σ [6]	5.14	4.99	4.82	5.21	5.19
Ca	1.70	1.99	2.05	1.86	1.69
Na	0.93	0.35	0.88	0.51	0.36
K	0.06	0.59	0.19	0.06	0.08

Note: I-P, Iratsu paragasite analyzed by electron microprobe. E-P, Einstödingen pargasite; combination by electron microprobe and wet-chemical analyses (Matsubara and Motoyoshi, 1985). O-H, Obira hastingsite analyzed by wet-chemical methods (Matsumoto and Miyashita, 1960). P-P, Parau pargasite analyzed by wet-chemical methods (Tomita, 1965). K-H, Kawanabe hornblende analyzed by electron microprobe.

* The amount of Fe^{3+} per formula unit in amphibole was derived from the total occupancy of Na and K in the A site determined by refinement (after Hawthorne et al., 1980).

tahedral sites in hornblendes formed at different temperatures.

SPECIMENS EXAMINED

The following five specimens were examined. Chemical compositions are given in Table 1, along with the methods of analyses for each specimen.

Iratsu pargasite (I-P)

Iratsu pargasite is one of the constituent minerals of the basic granulite from the Iratsu epidote-amphibolite

mass, emplaced in Sanbagawa schists, in Ehime Prefecture, Japan. The associated minerals are hypersthene, augite, and plagioclase. The pargasite crystallized in the granulite facies [750 °C and 5–10 kbar, as estimated by Yokoyama (1980)] and suffered Sanbagawa metamorphism [epidote amphibolite facies; about 600 °C and 8–13 kbar, as estimated by Yokoyama (1980) and Takasu (1984)]. The pargasite is slightly poorer in Mg and Al than the Einstödingen sample described below.

Einstödingen pargasite (E-P)

The pargasite occurs in a skarn intercalated with garnet biotite gneisses in an islet of Einstödingen, Lützow Holm Bay, East Antarctica (Matsubara and Motoyoshi, 1985). The studied specimen was supplied by Dr. Matsubara. The skarn consists of aluminous diopside, potassian pargasite, and phlogopite. The pargasite is the product of granulite-facies metamorphism. The metamorphic temperature and pressure were estimated to be about 800–850 °C and 8–10 kbar on the basis of the clinopyroxene-orthopyroxene geothermometer (Wood and Banno, 1973; Wells, 1977) and the garnet-orthopyroxene geobarometer (Harley and Green, 1982) by Matsubara and Motoyoshi (1985). The pargasite shows a high K content and Mg/(Mg + Fe²⁺). It contains high [6]Al (0.97 pfu).

Obira hastingsite (O-H)

The hastingsite was from a skarn in the Obira mine, Oita Prefecture, Japan. Chemistry and occurrence of the hastingsite were described in detail by Matsumoto and Miyashita (1960). The hastingsite is fibrous. Associated minerals are datolite and stilpnomelane, which crystallized later than other skarn minerals (garnet, wollastonite, hedenbergite, actinolite). Judging from the assemblage of skarn and ore-forming minerals, the hastingsite crystallized during the hydrothermal stage (Matsumoto and Miyashita, 1960). The hastingsite has a high Fe²⁺/(Mg + Fe²⁺) and contains little Al in the octahedral sites.

Parau pargasite (P-P)

This pargasite was found in andesitic agglomerate belonging to the Babeldaob agglomerate in Gapson, Parau Island (Tayama, 1939). The Babeldaob agglomerate intercalates limestone, shale, sandstone, and tuff, suggesting submarine deposition. The andesitic agglomerate contains pargasite, clinopyroxene, and plagioclase. The crystallization temperature of the pargasite was estimated to

TABLE 2. Crystal data for the hornblendes, space group $C2/m$

	I-P	E-P	O-H	P-P	K-H
a (Å)	9.805(3)	9.900(2)	9.967(4)	9.834(4)	9.829(8)
b (Å)	17.96(1)	17.95(2)	18.269(2)	18.01(3)	18.06(1)
c (Å)	5.302(1)	5.311(2)	5.347(1)	5.297(2)	5.304(1)
β (°)	104.93(2)	105.42(2)	104.97(2)	105.04(2)	104.70(2)
V (Å³)	902.1(8)	910.5(9)	940.05(9)	906.0(4)	910.2(8)
Size (mm)	0.15 × 0.10 × 0.25	0.15 × 0.10 × 0.30	0.15 × 0.10 × 0.50	0.30 × 0.20 × 0.50	0.20 × 0.10 × 0.30
R (weighted)	0.037	0.049	0.057	0.058	0.076
No. of F	2234	2967	1344	2701	2234

be about 900 °C, on the basis of the phase relations in tonalite (Wyllie, 1977). The pargasite shows a high Mg/(Mg + Fe²⁺) and is enriched in $^{[6]}$Al (0.96 pfu) (Tomita, 1965). Chemically, this pargasite and the Einstödingen pargasite are very similar to each other (Table 1).

Kawanabe hornblende (K-H)

The magnesio-hornblende was from phenocrysts of andesitic agglomerate collected in the Kawanabe area of Kagoshima Prefecture, Japan. The agglomerate contains hornblende, clinopyroxene, and plagioclase. This mineral assemblage gives about 900 °C as the crystallization temperature of the hornblende (Wyllie, 1977). The hornblende has a similar Mg/(Mg + Fe²⁺) to Einstödingen and Parau pargasites (Table 1). However the $^{[6]}$Al content is very low.

Comparison of the five specimens

Neither exsolution texture nor chemical zoning was observed in the five hornblendes by optical microscopy, X-ray photographs, and electron-microprobe analyses. The hornblendes show various Mg/(Fe²⁺ + Mg) ratios and contain more than 0.70 Al, Fe³⁺, and Ti pfu in the octahedral sites. They can be divided into two groups based on their occurrences: One group consists of Obira hastingsite, Iratsu pargasite, and Einstödingen pargasite; the other group, Parau pargasite and Kawanabe hornblende. The three hornblendes in the former group, which crystallized under metamorphic or hydrothermal conditions, are considered to have cooled slowly. Thus, intersite cation migration may have continued somewhat below the crystallization temperature. On the other hand, the two hornblendes in the latter group, which crystallized at much higher temperature and may have been cooled rapidly after volcanic eruption, are expected to preserve intracrystalline equilibrium frozen at a higher temperature than the former three hornblendes. Therefore, the former are considered to be "low-temperature" hornblendes, and the latter "high-temperature" hornblendes.

EXPERIMENTAL DETAILS

The crystals, usually {110} cleavage flakes elongated along the c axis, were hand-picked. The crystal sizes are shown in Table 2. The single-crystal X-ray photographs showed diffraction symmetry of space group Cm, C2 or C2/m. Since there was no indication of a noncentric nature from the intensity distribution, the space group C2/m was used in the structure refinements.

The intensity data were collected on a RIGAKU AFC-5UD automatic 4-circle diffractometer. The unit-cell parameters were determined by the least-squares method from 20 reflections collected on a 4-circle single-crystal diffractometer. Intensity data were measured with the 2θ-ω scan equi-inclination technique using monochromatized MoKα radiation and were gathered to 2θ = 80° for Obira hastingsite and to 2θ = 100° for the others. Absorption effects

were corrected by the semiempirical method of North et al. (1968). Intensities less than three times the standard deviation of the observed intensity were rejected in this refinement.

The cell parameters, crystal sizes, number of intensity measurements, and the final $R = \Sigma||F_{obs}| - |F_{calc}||/\Sigma|F_{obs}|$ are presented in Table 2.

Refinement procedure

The full matrix least-squares refinements were carried out by using the computer program RFINE IV (Finger and Price, 1975) revised by Horiuchi (personal communication, 1981). The initial positional parameters and isotropic temperature factors for the present refinements were taken from ferro-tschermakite (Hawthorne and Grundy, 1973).

Since the X-ray scattering power of Mg and Al atoms is indistinguishable, Mg and Al were regarded as one group with one scattering factor. Mg and Al atoms were summed to form Mg* in atomic fraction. For the same reason, Fe²⁺, Fe³⁺, and Ti were assumed to form a species, Fe*. The small amount of Mn in the five hornblendes was neglected in this refinement. Because of the chemical complexity of hornblende, the following simplifying assumptions were employed. Ca was constrained to the M(4) site, excess cations (Fe* and Mg*) for the octahedral sites in Iratsu pargasite, Parau pargasite, and Kawanabe hornblende were assigned to the M(4) site, and the rest of the site was filled with Na. The M(4) sites of Einstödingen pargasite and Obira hastingsite were filled with Ca and Na. Residual Na and K were assigned to the A site.

Assuming random distribution of Al and Si in the tetrahedral sites and of Mg* and Fe* in the octahedral sites and/or the M(4) site, initial site occupancies were determined from the chemical analyses.

During all cycles of refinements, the tetrahedral and octahedral site chemistry were constrained to agree with the chemical analyses. Positional disorder of the A site on the mirror plane and/or along the twofold axis was read from the Fourier and difference-Fourier sections. Split-atom models (Papike et al., 1969; Hawthorne and Grundy, 1973) were used, which reduced the R factor more than 1.0%. The total amount of Na and K in the A site of Iratsu pargasite and Kawanabe hornblende was determined, assuming random distribution of Na and K cations in the A site. The anisotropic temperature factors were refined for Iratsu, Einstödingen, and Parau pargasites, for which the final weighted R factors are 3.1, 4.1, and 4.7%, respectively. In Iratsu pargasite, Parau pargasite, and Kawanabe hornblende, Mg* and Fe* at the M(4) site are Mg and Fe²⁺, respectively.

From the chemical analyses and X-ray refinements, Si and Al occupancies in the tetrahedral sites and Mg* and Fe* occupancies in the octahedral sites and/or the M(4) site were determined. The final positional parameters, isotropic temperature factors, and site occupancies are listed in Tables 3 and 4, respectively.

TABLE 3. Positional parameters and isotropic temperature factors for the hornblendes

		I-P	E-P	O-H	P-P	K-H
T(1)	x	0.2809(1)	0.2776(1)	0.2774(3)	0.2816(1)	0.2819(2)
	y	0.0858(1)	0.0863(1)	0.0846(2)	0.0852(1)	0.0848(1)
	z	0.3014(1)	0.3049(2)	0.2958(7)	0.3009(2)	0.2974(4)
	B	0.48(3)	0.44(3)	0.45(5)	0.39(2)	0.54(2)
T(2)	x	0.2919(1)	0.2961(1)	0.2915(3)	0.2914(1)	0.2909(2)
	y	0.1731(1)	0.1741(1)	0.1717(2)	0.1725(1)	0.1717(1)
	z	0.8133(2)	0.8162(2)	0.8089(7)	0.8113(2)	0.8063(4)
	B	0.48(2)	0.47(3)	0.52(4)	0.39(2)	0.54(2)
M(1)	x	0.0	0.0	0.0	0.0	0.0
	y	0.0886(1)	0.0903(1)	0.0915(1)	0.0879(1)	0.0873(1)
	z	0.5	0.5	0.5	0.5	0.5
	B	0.78(2)	0.92(3)	0.53(4)	0.67(2)	0.95(3)
M(2)	x	0.0	0.0	0.0	0.0	0.0
	y	0.1772(1)	0.1768(1)	0.1787(1)	0.1768(1)	0.1774(1)
	z	0.0	0.0	0.0	0.0	0.0
	B	0.49(2)	0.63(3)	0.37(4)	0.41(2)	0.74(3)
M(3)	x	0.0	0.0	0.0	0.0	0.0
	y	0.0	0.0	0.0	0.0	0.0
	z	0.0	0.0	0.0	0.0	0.0
	B	0.62(2)	0.87(2)	0.38(5)	0.47(2)	0.87(4)
M(4)	x	0.0	0.0	0.0	0.0	0.0
	y	0.2789(1)	0.2809(1)	0.2806(1)	0.2785(1)	0.2768(1)
	z	0.5	0.5	0.5	0.5	0.5
	B	0.80(3)	0.67(5)	0.91(5)	0.91(1)	0.97(2)
A(m)	x	0.0474(25)	0.0203(40)	0.0365(24)	0.0292(27)	0.0
	y	0.5	0.5	0.5	0.5	0.5
	z	0.1014(50)	0.0426(80)	0.0472(60)	0.1245(61)	0.0
	B	2.70(31)	1.73(31)	1.74(52)	2.48(30)	3.44(36)
A(2)	x	0.0		0.0	0.0	
	y	0.4774(7)		0.4756(18)	0.4793(5)	
	z	0.0		0.0	0.0	
	B	2.16(56)		1.93(55)	2.36(45)	
O(1)	x	0.1070(2)	0.1045(2)	0.1048(7)	0.1074(2)	0.1110(4)
	y	0.0896(1)	0.0902(1)	0.0896(4)	0.0874(1)	0.0873(2)
	z	0.2145(5)	0.2148(5)	0.2116(16)	0.2160(5)	0.2186(8)
	B	0.95(3)	0.83(4)	0.55(10)	0.79(3)	0.76(6)
O(2)	x	0.1204(2)	0.1204(2)	0.1227(7)	0.1197(2)	0.1204(4)
	y	0.1742(1)	0.1750(1)	0.1763(4)	0.1733(1)	0.1727(2)
	z	0.7366(4)	0.7375(5)	0.7297(17)	0.7316(4)	0.7279(8)
	B	0.77(3)	0.82(4)	0.76(13)	0.63(3)	0.77(6)
O(3)	x	0.1101(3)	0.1123(3)	0.1235(13)	0.1087(3)	0.1114(6)
	y	0.0	0.0	0.0	0.0	0.0
	z	0.7140(7)	0.7151(7)	0.7140(30)	0.7157(7)	0.7158(12)
	B	0.86(5)	0.76(5)	1.14(24)	0.84(4)	0.83(8)
O(4)	x	0.3684(2)	0.3687(2)	0.3661(8)	0.3672(2)	0.3673(4)
	y	0.2501(1)	0.2506(1)	0.2478(4)	0.2497(1)	0.2485(2)
	z	0.7895(5)	0.7934(5)	0.7893(18)	0.7875(5)	0.7896(9)
	B	0.92(3)	0.87(4)	1.04(12)	0.90(3)	1.04(6)
O(5)	x	0.3500(2)	0.3491(2)	0.3442(8)	0.3495(2)	0.3473(4)
	y	0.1404(1)	0.1398(1)	0.1363(4)	0.1403(1)	0.1374(2)
	z	0.1084(5)	0.1129(5)	0.0991(18)	0.1100(5)	0.1012(8)
	B	0.88(3)	0.86(4)	1.05(12)	0.90(3)	0.90(6)
O(6)	x	0.3427(2)	0.3418(2)	0.3397(8)	0.3440(2)	0.3436(4)
	y	0.1181(1)	0.1186(1)	0.1198(4)	0.1165(1)	0.1188(2)
	z	0.6072(5)	0.6108(5)	0.5920(19)	0.6070(5)	0.5945(8)
	B	1.01(3)	0.92(4)	0.95(12)	0.99(3)	0.92(6)
O(7)	x	0.3380(3)	0.3344(3)	0.3299(10)	0.3393(3)	0.3367(6)
	y	0.0	0.0	0.0	0.0	0.0
	z	0.2765(7)	0.2880(7)	0.2928(25)	0.2745(7)	0.2839(12)
	B	1.23(5)	1.20(6)	1.10(17)	1.08(5)	0.87(9)

RESULTS

T(1) and T(2) tetrahedral sites

In the five hornblendes of this study, Al tends to occupy the T(1) site in preference to the T(2) site, as judged from the ⟨T(1)–O⟩ and ⟨T(2)–O⟩ bond lengths (Table 5). Iratsu, Einstödingen, and Parau pargasites and Obira hastingsite, rich in [4]Al (about 1.8–2.0 atoms pfu), have similar ⟨T(1)–O⟩ and also ⟨T(2)–O⟩ lengths. The ⟨T(1)–O⟩

TABLE 4. Site occupancies of the hornblendes

		I-P	E-P	O-H	P-P	K-H
T(1)	Si	0.57(8)	0.50(9)	0.58	0.60(8)	0.77(10)
	Al	0.43	0.50	0.42	0.40	0.23
T(2)	Si	0.98	0.99	1.00	0.89	0.96
	Al	0.02	0.01	0.0	0.11	0.04
M(1)	Mg*	0.615(3)	0.822(4)	0.06(1)	0.759(4)	0.676(4)
	Fe*	0.385	0.178	0.94	0.241	0.324
M(2)	Mg*	0.816(3)	0.838(3)	0.15(1)	0.763(4)	0.673(4)
	Fe*	0.184	0.162	0.85	0.237	0.327
M(3)	Mg*	0.481(3)	0.780	0.13	0.764(6)	0.664(3)
	Fe*	0.519	0.220	0.87	0.236(6)	0.336
M(4)	Ca	0.851	0.995	1.0	0.930	0.85
	Na	0.092	0.005			0.07
	Mg	0.0			0.011	0.04
	Fe^{2+}	0.057			0.059	0.04
A	Na + K	0.80(1)	0.94	0.99	0.57	0.32(2)

Note: Mg* = Mg + Al, Fe* = Fe^{2+} + Fe^{3+} + Ti.

TABLE 5. Interatomic distances (Å) in the hornblendes

		I-P	E-P	O-H	P-P	K-H
T(1)–O(1)	×1	1.649(2)	1.653(2)	1.664(7)	1.654(2)	1.624(4)
O(5)	×1	1.681(3)	1.688(3)	1.674(9)	1.675(3)	1.655(5)
O(6)	×1	1.681(3)	1.683(3)	1.673(9)	1.676(3)	1.657(5)
O(7)	×1	1.656(3)	1.660(1)	1.633(4)	1.654(2)	1.632(3)
Mean		1.667	1.671	1.661	1.665	1.642
T(2)–O(2)	×1	1.625(2)	1.625(2)	1.627(7)	1.631(2)	1.620(4)
O(4)	×1	1.594(2)	1.597(2)	1.593(8)	1.598(2)	1.591(4)
O(5)	×1	1.630(3)	1.647(3)	1.637(9)	1.642(3)	1.642(5)
O(6)	×1	1.643(3)	1.654(3)	1.662(10)	1.657(3)	1.655(5)
Mean		1.623	1.631	1.630	1.632	1.627
M(1)–O(1)	×2	2.052(3)	2.049(3)	2.074(9)	2.050(3)	2.060(5)
O(2)	×2	2.138(3)	2.127(2)	2.153(7)	2.123(2)	2.123(4)
O(3)	×2	2.086(3)	2.121(2)	2.210(8)	2.079(2)	2.088(4)
Mean		2.092	2.099	2.146	2.084	2.090
M(2)–O(1)	×2	2.062(3)	2.040(2)	2.100(7)	2.095(3)	2.130(4)
O(2)	×2	2.048(2)	2.061(3)	2.121(9)	2.069(3)	2.087(5)
O(4)	×2	1.969(3)	1.959(2)	2.019(7)	1.990(2)	2.000(4)
Mean		2.026	2.020	2.080	2.051	2.072
M(3)–O(1)	×4	2.090(3)	2.091(2)	2.107(7)	2.068(2)	2.093(4)
O(3)	×2	2.076(4)	2.103(4)	2.197(8)	2.061(4)	2.075(7)
Mean		2.085	2.095	2.137	2.066	2.087
M(4)–O(2)	×2	2.396(3)	2.414(2)	2.421(7)	2.393(3)	2.382(4)
O(4)	×2	2.305(3)	2.348(3)	2.347(10)	2.305(3)	2.299(5)
O(5)	×2	2.646(3)	2.618(2)	2.755(8)	2.648(3)	2.741(4)
O(6)	×2	2.564(3)	2.559(2)	2.552(8)	2.589(3)	2.560(4)
Mean		2.478	2.485	2.519	2.484	2.496
A(m)–O(5)	×2	3.002(15)	3.035(2)	3.059(18)	3.996(13)	3.018(4)
O(5)	×2	3.196(13)	3.155(2)	3.193(19)	3.231(11)	3.018(4)
O(6)	×2	2.700(14)	2.911(4)	2.981(20)	2.592(12)	3.148(4)
O(6)	×2	3.531(18)	3.264(4)	3.461(22)	3.633(16)	3.148(4)
O(7)	×1	2.499(27)	2.521(6)	2.517(35)	2.564(25)	2.463(7)
O(7)	×1	3.250(25)	3.487(6)	2.697(33)	3.100(22)	3.730(6)
O(7)	×1	2.483(24)	2.519(6)	3.454(33)	2.463(22)	2.463(7)
O(7)	×1	4.277(24)	3.931(6)	4.013(31)	4.435(22)	3.730(6)
Mean		3.115	3.099	3.161	3.180	3.089
A(2)–O(5)	×2	2.699(10)		2.708(26)	2.753(8)	
O(5)	×2	3.412(12)		3.433(29)	3.386(8)	
O(6)	×2	2.813(8)		2.923(21)	2.822(6)	
O(6)	×2	3.403(10)		3.529(26)	3.345(7)	
O(7)	×2	2.461(4)		2.621(14)	2.437(4)	
O(7)	×2	3.778(4)		3.753(13)	3.776(6)	
Mean		3.095		3.161	3.087	

length of Kawanabe hornblende containing 1.1 pfu of [4]Al is shorter than those of the pargasites and hastingsite of this study.

The M(1), M(2), and M(3) octahedral sites

The site refinements (Table 4) of the Iratsu pargasite and Obira hastingsite indicate that the M(2) site is enriched in Mg* over the M(1) and M(3) sites. The M(1), M(2), and M(3) sites in Einstödingen and Parau pargasites as well as in Kawanabe hornblende contain almost randomly distributed Mg* and Fe*.

Similar to other hornblendes reported by previous authors, the ⟨M(2)–O⟩ length of these five hornblendes is less than the ⟨M(1)–O⟩ and ⟨M(3)–O⟩ lengths (Table 5). In particular, the differences between the ⟨M(2)–O⟩ length and the ⟨M(1)–O⟩ and ⟨M(3)–O⟩ lengths are large (more than 0.06 Å) in Iratsu pargasite, Einstödingen pargasite, and Obira hastingsite but not so large (less than 0.03 Å) in Parau pargasite and Kawanabe hornblende. Einstödingen and Parau pargasite with comparable Al and Fe^{3+} in the octahedral sites are considerably different in the mean bond length of the M(2) site (2.020 and 2.051 Å, respectively).

The thermal ellipsoids of the octahedral sites in Iratsu, Einstödingen, and Parau pargasites are similar in the orientation and the magnitudes (0.6–1.1) of their principal axes.

The M(4) polyhedral site

The M(4) sites of Einstödingen pargasite and Obira hastingsite are filled with Ca and Na cations. In Iratsu and Parau pargasites, the M(4) sites prefer Fe^{2+} over Mg. The M(4) site in Kawanabe hornblende contains equal proportions of Mg and Fe^{2+}.

The A site

The positional disorder of the A site occurs on the mirror plane in the five hornblendes and also along the twofold axis, except for Einstödingen pargasite and Kawan-

abe hornblende. The A(m) sites on the mirror plane shift less than about 0.3 Å from the center position (2/m position) in the five hornblendes. The displacement of the A(2) site along the twofold axis is also less than about 0.3 Å from the center position (2/m).

CATION OCCUPANCY IN THE OCTAHEDRAL SITES

Robinson et al. (1973) and Hawthorne (1978, 1981, 1983) developed a relationship between the mean bond length and mean ionic radius [which is the mean of the effective radius of the constituent cations (Shannon and Prewitt, 1969, 1970)] for the octahedral sites in clinoamphiboles. This relationship can be used to characterize unknown site occupancies or to test the obtained site occupancies.

Relation between the mean ionic radius and mean bond length for the grand octahedral site

The grand ⟨M–O⟩ length, which is the mean of the ⟨M(1)–O⟩, ⟨M(2)–O⟩, and ⟨M(3)–O⟩ lengths, increases
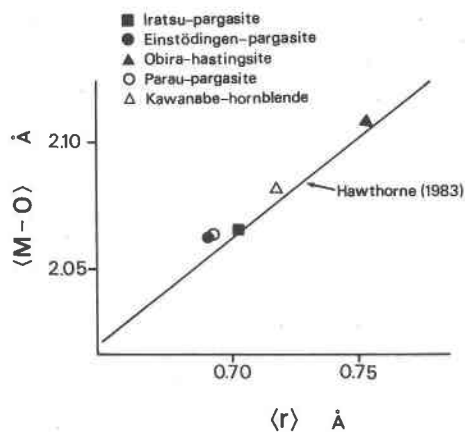
Fig. 1. Plot of the grand mean bond length of the octahedral site versus the mean ionic radius of the constituent cations in the hornblendes. All data of the studied hornblendes are consistent with the relation shown by a solid line derived from other $C2/m$ amphiboles (Hawthorne, 1983).

Fig. 2. Plot of the $\langle M(2)–O\rangle$ length versus the mean ionic radius of the $M(2)$ site for the hornblendes. Al, Fe^{3+}, and Ti cations are assumed to be located in the $M(2)$ site. In this relation, Obira hastingsite and Iratsu and Einstödingen pargasites are in agreement with the correlation shown by a solid line (Hawthorne, 1983), but Parau pargasite and Kawanabe hornblende are not. Symbols as in Fig. 1.

linearly with the mean ionic radius of the constituent cations in these octahedral sites in $C2/m$ amphiboles (Hawthorne, 1981, 1983). As is obvious in Figure 1, the data of the five hornblendes in the present investigation are consistent with the correlation line.

Relation between the mean ionic radius and mean bond length for the individual octahedral sites

Whittaker (1949) suggested on account of the significantly short $\langle M(2)–O\rangle$ length compared to the $\langle M(1)–O\rangle$ and $\langle M(3)–O\rangle$ lengths that trivalent cations in magnesioriebeckite are concentrated in the $M(2)$ site. Using the same reasoning, other workers (Papike and Clark, 1968; Robinson et al., 1973; Hawthorne, 1978) showed that Al, Fe^{3+}, and Ti may be concentrated in the $M(2)$ site in clinoamphiboles. Furthermore, Robinson et al. (1973) demonstrated a linear relationship between the mean bond length and the mean ionic radius in the octahedral sites of hornblendes. Such a correlation line was developed separately for individual octahedral sites by Hawthorne (1978, 1981, 1983), using a larger data set of the $C2/m$
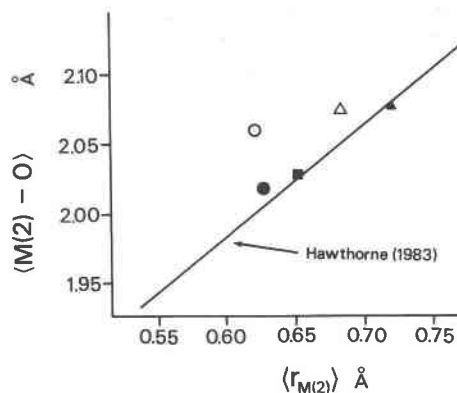
amphiboles. He suggested that the relation holds good for the $M(2)$ site, but not for the $M(1)$ and $M(3)$ sites. The assignment of Al, Fe^{3+}, and Ti to the individual octahedral sites is examined here in the five hornblendes of this study, relying mainly on the correlation line for the $M(2)$ site.

Shortness of the $\langle M(2)–O\rangle$ length relative to the $\langle M(1)–O\rangle$ and $\langle M(3)–O\rangle$ lengths suggests that smaller Al, Fe^{3+}, and Ti cations are segregated into the $M(2)$ site in the five hornblendes. Thus, Al, Fe^{3+}, and Ti in the octahedral sites were assumed to occupy the $M(2)$ site, where the residual fractions of Mg* and Fe* are Mg and Fe^{2+}, respectively. The refined Mg* and Fe* occupancies in the $M(1)$ and $M(3)$ sites were converted to the Mg and Fe^{2+} occupancies, respectively. The $\langle M(2)–O\rangle$ length was plotted against the mean ionic radius derived from the occupancy of the $M(2)$ site to be compared with the correlation line of the mean bond length versus the mean ionic radius (Fig. 2). Obira hastingsite and Iratsu and Einstödingen pargasites are consistent with the correlation line, whereas Parau pargasite and Kawanabe hornblende deviate from the line of the $M(2)$ site, i.e., the latter two hornblendes have observed $\langle M(2)–O\rangle$ lengths that are larger than the lengths calculated from the mean ionic radius by using the correlation line of the $M(2)$ site (Hawthorne, 1983). In the same manner, the observed mean bond lengths and those calculated by Hawthorne's equations (Hawthorne, 1983) also disagree with each other for the $M(1)$ and $M(3)$ sites of the two hornblendes. The differences between the observed and calculated mean bond lengths of the $M(1)$, $M(3)$, and $M(2)$ sites are shown in Table 6 for Parau pargasite and Kawanabe hornblende. Their observed grand $\langle M–O\rangle$ lengths, however, are consistent with the calculated ones. Hence the positive value of $\langle M(2)–O\rangle_{obs} - \langle M(2)–O\rangle_{calc}$ tends to be compensated by the negative values of the differences for the $M(1)$ and

TABLE 6. Observed and calculated mean bond lengths (Å) of the octahedral sites

	Observed	Calculated*	Calculated**
Parau pargasite			
M(1,3)	2.078	2.097	2.070
M(2)	2.051	1.998	2.041
Kawanabe hornblende			
M(1,3)	2.089	2.098	2.088
M(2)	2.072	2.052	2.068

Note: The calculated values were obtained by Hawthorne's equations (Hawthorne, 1983). The M(1,3) values are the average of the M(1) and M(3) sites.
* Al, Fe^{3+}, and Ti are assigned to the M(2) site.
** After re-arrangement (see Table 7).

TABLE 7. Octahedral site occupancies of the hornblendes

		I-P	E-P	O-H	P-P	K-H
M(1)	Mg	0.615	0.822	0.06	0.62	0.66
	Fe^{2+}	0.385	0.178	0.94	0.19	0.26
	Al				0.14	0.02
	Fe^{3+}				0.05	0.06
M(2)	Mg	0.456	0.353	0.13	0.49	0.62
	Fe^{2+}	0.067	0.027	0.45	0.13	0.14
	Al	0.360	0.485	0.02	0.27	0.05
	Fe^{3+}	0.024	0.110	0.36	0.11	0.12
	Ti	0.093	0.025	0.04		0.07
M(3)	Mg	0.481	0.780	0.13	0.62	0.64
	Fe^{2+}	0.519	0.220	0.87	0.19	0.28
	Al				0.14	0.02
	Fe^{3+}				0.05	0.06

Note: Re-arrangements maintained refined occupancies (see Table 4).

Fig. 3. Mg-Fe^{2+} distribution between the M(1) and M(3) sites in the hornblendes. Solid line: $K_D^{M(1)-M(2)} = 1.0$. + symbol: ferro-tschermakite (Hawthorne and Grundy, 1973). x symbol: pargasitic hornblende (Hawthorne et al., 1980). Other symbols as in Fig. 1.

M(3) sites (Table 6). It follows that the foregoing assignment of Al, Fe^{3+}, and Ti to the M(2) site is not adequate in Parau pargasite and Kawanabe hornblende. The disagreement in the calculated and observed mean bond lengths of the two hornblendes arises from overestimation of the amounts of smaller Al, Fe^{3+}, and Ti cations in the M(2) site and from underestimation of the amounts of smaller cations in the M(1) and M(3) sites.

Re-arrangement of cation occupancies in the octahedral sites

From the above discussion, Al, Fe^{3+}, and Ti appear to be located only at the M(2) site in Obira hastingsite and Iratsu and Einstödingen pargasites. Their site occupancies are listed in Table 7.

The optimum arrangements of Al, Fe^{3+}, and Ti cations within the octahedral sites for Parau pargasite and Kawanabe hornblende were estimated so that the mean ionic radius of each octahedral site was close to the calculated one from the observed mean bond length by Hawthorne's equations (Hawthorne, 1983) under the following constraints. The refined Mg* and Fe* fractions of every site were retained. Total contents of Al and Fe^{3+} over the octahedral sites were constrained to agree with the chemical analyses. Every octahedral site was assumed to contain the same Al/Fe^{3+} as the ratio obtained by chemical analyses. The M(1) and M(3) sites were treated as one set. Ti, which is small in amount in the octahedral site, was assigned to the M(2) site. The cation occupancies of the octahedral sites determined in this way are presented in Table 7.

Thermal ellipsoids of Iratsu, Einstödingen, and Parau pargasites show no evidence of positional disorder in the octahedral sites. Therefore, there is no problem in using the relations between the mean bond length and ionic radius for the examined hornblendes.

CATION ORDER-DISORDER AMONG THE OCTAHEDRAL SITES IN HORNBLENDE

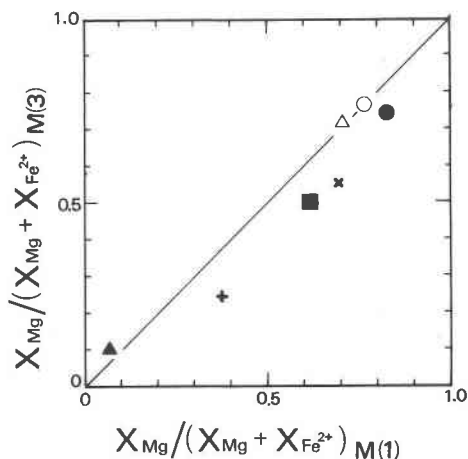On the basis of their occurrences, the five hornblendes can be divided into two groups: "high-temperature" and "low-temperature" ones from metamorphic rocks and skarn. The nonconvergent cation order-disorder among the octahedral sites will be discussed here for the five hornblendes as well as for a ferro-tschermakite (Hawthorne and Grundy, 1973) and a pargasitic hornblende (Hawthorne et al., 1980). The ferro-tschermakite occurred in the Frood mine, Sudbury, Canada, and the pargasitic hornblende occurred in an amphibolite sequence at the margin of Tallan Lake sill, Peterborough County, Ontario. The two hornblendes are considered to belong to the "low-temperature" hornblendes because they are of metamorphic origin.

Mg-Fe^{2+} order-disorder among the octahedral sites

Figure 3 is a plot of the Mg/(Mg + Fe^{2+}) of the M(1) site against that of the M(3) site. The Mg-Fe^{2+} distribution constant between the M(1) and M(3) sites is given by

$$K_D^{M(1)-M(3)} = \left(\frac{X_{Mg}}{X_{Fe^{2+}}}\right)_{M(3)} \Bigg/ \left(\frac{X_{Mg}}{X_{Fe^{2+}}}\right)_{M(1)}, \quad (1)$$

where X is the atomic fraction in the sites.

$K_D^{M(1)-M(3)}$ is about 0.6 for "low-temperature" hornblendes except for Obira hastingsite and is nearly unity for "high-temperature" hornblendes.

The Mg-Fe^{2+} distribution between the M(2) and the M(1) sites is shown in Figure 4. The distribution constant between the M(2) and M(1) sites is given by

$$K_D^{M(1)-M(2)} = \left(\frac{X_{Mg}}{X_{Fe^{2+}}}\right)_{M(1)} \Bigg/ \left(\frac{X_{Mg}}{X_{Fe^{2+}}}\right)_{M(2)}, \quad (2)$$

where X is the atomic fraction in the sites.
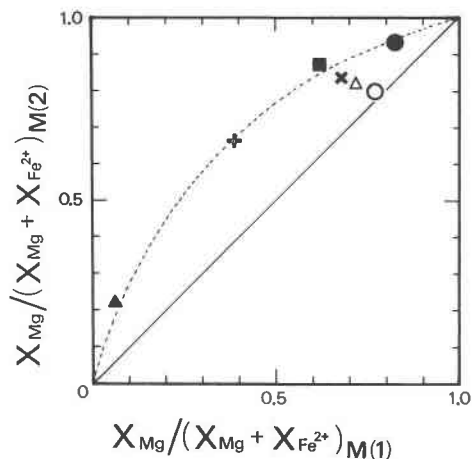
"Low-temperature" hornblendes plot near the curve

Fig. 4. Mg-Fe^{2+} distribution between the M(2) and M(1) sites in the hornblendes. Solid line: $K_D^{M(1)-M(2)} = 1.0$. Broken line: $K_D^{M(1)-M(2)} = 0.3$. Symbols as in Figs. 1 and 3.

for $K_D^{M(1)-M(2)} = 0.3$. "High-temperature" hornblendes, especially Parau pargasite, plot near the curve for $K_D^{M(1)-M(2)} = 1.0$ and thus indicate little preference for ordering of Mg and Fe^{2+} between the M(1) and M(2) sites. So "low-temperature" hornblendes show the Mg/Fe^{2+} to be M(2) $\gg$ M(1) > M(3). At high temperature, the octahedral sites of hornblendes may become indistinguishable from each other for the Mg and Fe^{2+} cations.

The Mg-Fe^{2+} partitioning coefficient between the M(4) and M(1, 2, 3) of metamorphic cummingtonites is 0.02–0.08 (Ghose and Weidner, 1972). Geometrically the M(2), M(1), and M(3) sites of clinoamphibole are more or less similar sites, but the M(4) site differs much from the octahedral sites in size and coordination number. Accordingly, it is reasonable that the $K_D^{M(1)-M(2)}$ (0.3) between the M(1) and M(2) sites is larger than that between the M(4) and M(1, 2, 3) sites.

Al-Fe^{3+} order-disorder among the octahedral sites

Concentration of Al, Fe^{3+}, and Ti into the M(2) site in the "low-temperature" hornblendes was discussed above. In "high-temperature" hornblendes, the observed mean bond lengths of the octahedral sites suggest that Al and Fe^{3+} are located not only in the M(2) site but also the M(1) and M(3) sites with some preference for the M(2) site. In "high-temperature" hornblendes, Al and Fe^{3+} tend to distribute over the octahedral sites along with random distribution of Mg and Fe^{2+}.

The cation distribution in cummingtonite from volcanic rocks indicates a temperature much lower than the crystallization temperature (Ghose and Weidner, 1972; Buckley and Wilkins, 1971). A similar phenomenon was expected for hornblendes, but the fact that "high-temperature" hornblendes in this study preserve disordered cation distribution suggests their rapid quenching from higher crystallization temperature. The cummingtonite studied by Buckley and Wilkins (1971) was from lavas, but the "high-temperature" hornblendes of this study are from agglomerate deposited on the sea floor. The rapid quenching in sea water may be responsible for the preservation of the random distribution of cations in "high-temperature" hornblendes.

Similar disordering of divalent and trivalent cations in the octahedral sites of experimentally oxidized tshermakitic hornblende and riebeckite was reported by Phillips et al. (1988). Al and Fe^{3+} migrate from the M(2) site to the M(1) and M(3) sites of the riebeckite [O(3) = 0.10(OH) + 0.90(O)] heated in air. Parau pargasite [O(3) = 0.71(OH) + 0.29(O)], in which Al and Fe^{3+} are distributed over the octahedral sites, is different from the riebeckite in the degree of oxidation. Thus, cation disordering in the octahedral site of amphibole is considered to depend on the crystallization temperature as well as on the oxidation degree of hornblende. Which is the most important factor in the cation disordering is not known. Further examinations will be needed to make it clear.

CONCLUSION

The structure refinements of the "high- and low-temperature" hornblendes have been carried out. The mean bond lengths and the calculated mean ionic radius of the octahedral sites in the "low-temperature" hornblendes are consistent with the equation proposed by Hawthorne (1983). However the "high-temperature" hornblendes are inconsistent with that relation. The inconsistency arises mainly from the assignment of Al and Fe^{3+} only to the M(2) site, thereby suggesting that the conventional method of assignment is unsuitable for the "high-temperature" hornblendes. Therefore, cation distributions among the octahedral sites were estimated so as to be consistent with the refined mean bond lengths, on the basis of the relation between mean ionic radius and mean bond length.

At low temperature, such as metamorphic and hydrothermal conditions, Al, Fe^{3+}, and Ti are ordered on the M(2) site, and Mg exhibits a preference, M(2) $\gg$ M(1) > M (3), $K_D^{M(1)-M(2)} = 0.3$, for occupancy of the M(2) and M(1) sites. On the other hand, hornblendes from the volcanic rocks show more disordered cation distributions among the octahedral sites than hornblendes from metamorphic rocks and skarn.

REFERENCES CITED

Buckley, A.N., and Wilkins, R.W.T. (1971) Mössbauer and infrared study of a volcanic amphibole. American Mineralogist, 56, 90–100.
Finger, L.W., and Price, E. (1975) A system of Fortran IV computer programs for crystal structure computations. National Bureau of Standards Technical Note 854.
Ghose, S., and Weidner, J.R. (1972) Mg^{2+}-Fe^{2+} order-disorder in cum-

mingtonite, $(Mg,Fe)_7Si_8O_{22}(OH)_2$: A new geothermometer. Earth and Planetary Science Letters, 16, 346–354.

Hafner, S.S., and Ghose, S. (1971) Iron and magnesium distribution in cummingtonites $(Fe,Mg)_7Si_8O_{22}(OH)_2$. Zeitschrift für Kristallographie, 133, 301–326.

Harley, S.L., and Green, D.H. (1982) Garnet-orthopyroxene barometry for granulites and peridotites. Nature, 300, 697–701.

Hawthorne, F.C. (1978) The crystal chemistry of the amphiboles. VI. The stereo chemistry of the octahedral strip. Canadian Mineralogist, 16, 37–52.

—— (1981) Crystal chemistry of the amphiboles. Mineralogical Society of America Reviews in Mineralogy, 9A, 1–102.

—— (1983) The crystal chemistry of the amphiboles. Canadian Mineralogist, 21, 173–480.

Hawthorne, F.C., and Grundy, H.D. (1973) The crystal chemistry of the amphiboles. I. Refinement of the crystal structure of ferrotschermakite. Mineralogical Magazine, 39, 36–48.

—— (1977) The crystal chemistry of the amphiboles. III. Refinement of the crystal structure of a subsilicic hastingsite. Mineralogical Magazine, 41, 43–51.

Hawthorne, F.C., Griep, J.L., and Curtis, L. (1980) A three-amphibole assemblage from the Tallan Lake sill, Peterborough County, Ontario. Canadian Mineralogist, 18, 275–284.

Kitamura, M., Tokonami, M., and Morimoto, N. (1975) Distribution of titanium atoms in oxy-kaersutite. Contributions to Mineralogy and Petrology, 51, 167–172.

Leake, B.E. (1978) Nomenclature of amphiboles. American Mineralogist, 63, 1023–1052.

Matsubara, S., and Motoyoshi, Y. (1985) Potassium pargasite from Einstödingen, Lützow-Holm Bay, East Antarctica. Mineralogical Magazine, 49, 703–707.

Matsumoto, Y., and Miyashita, M. (1960) Ferrohastingsite from the Obira mine, Kyushu, Japan. Journal of the Mineralogical Society of Japan, 4, 372–382 (in Japanese with English abstract).

Mueller, R.F. (1962) Energetics of certain silicate solid solutions. Geochimica et Cosmochimica Acta, 26, 581–598.

North, A.C.T., Phillips, D.C., and Mathews, F.S. (1968) A semi-empirical method of absorption correction. Acta Crystallographica, A24, 351–359.

Papike, J.J., and Clark, J.R. (1968) The crystal structure and cation distribution of glaucophane. American Mineralogist, 53, 1156–1173.

Papike, J.J., Ross, M., and Clark, J.R. (1969) Crystal-chemical characterization of clinoamphiboles based on five new structure refinements. Mineralogical Society of America Special Paper 2, 117–136.

Phillips, M.W., Popp, R.K., and Clowe, C.A. (1988) Structure adjustment accompanying oxidation-dehydrogenation in amphiboles. American Mineralogist, 73, 500–506.

Robinson, K., Gibbs, G.V., Ribbe, P.H., and Hall, M.R. (1973) Cation distribution in three hornblendes. American Journal of Science, 273A, 522–535.

Seifert, F., and Virgo, D. (1975) Kinetics of the Fe^{2+}-Mg, order-disorder reaction in anthophyllites: Quantitative cooling rates. Science, 188, 1107–1109.

Shannon, R.D., and Prewitt, C.T. (1969) Effective ionic radii in oxides and fluorides. Acta Crystallographica, B25, 925–946.

—— (1970) Revised values of effective ionic radii. Acta Crystallographica, B26, 1046–1048.

Shido, F., and Miyashiro, A. (1959) Hornblendes of basic metamorphic rocks. Journal of Faculty of Science, University of Tokyo, 12, 85–102.

Takasu, A. (1984) Prograde and retrograde eclogite in Sanbagawa metamorphic belt in Besshi district, Japan. Journal of Petrology, 25, 619–643.

Tayama, R. (1939) Geology and mineral resources in Babeldaob (of Parau) islands. Bulletin of the Tropical Industry Institute of Parau, South Sea Islands, Japan, 3, 1–19 (in Japanese).

Tomita, K. (1965) Studies on oxyhornblende. Memoirs of the College of Science, University of Kyoto, Series B, 32, 47–87.

Ungaretti, L., Smith, D.C., and Rossi, G. (1981) Crystal-chemistry by X-ray structure refinement and electron microprobe analysis of a series of sodic-calcic to alkali-amphiboles from the Nybö eclogite pod, Norway. Bulletin de la Société Française de Minéralogie et de Cristallographie, 104, 400–412.

Warren, B.E. (1929) The structure of tremolite $H_2Ca_2Mg_5(SiO_3)_8$. Zeitschrift für Kristallographie, 72, 42–57.

—— (1930) The crystal structure and chemical composition of the monoclinic amphiboles. Zeitschrift für Kristallographie, 72, 493–517.

Wells, P.R.A. (1977) Pyroxene thermometry in simple and complex systems. Contributions to Mineralogy and Petrology, 62, 129–139.

Whittaker, E.J.W. (1949) The structure of Bolivian crocidolite. Acta Crystallographica, 2, 312–317.

Wood, B.J., and Banno, S. (1973) Garnet-orthopyroxene and orthopyroxene-clinopyroxene relationships in simple and complex systems. Contributions to Mineralogy and Petrology, 42, 109–124.

Wyllie, P.J. (1977) Crustal anatexis: An experimental review. Tectonophysics, 43, 41–71.

Yamaguchi, Y., Shibakusa, H., and Tomita, K. (1983) Exsolution of cummingtonite, actinolite and sodic amphiboles in hornblende in high-pressure metamorphism. Nature, 304, 257–259.

Yokoyama, K. (1980) Nikubuchi peridotite body in the Sanbagawa metamorphic belt; thermal history of the "Al-pyroxene–rich suite" peridotite body in high pressure metamorphic terrain. Contributions to Mineralogy and Petrology, 73, 1–13.